HHS Public Access

Author manuscript

Cancer Lett. Author manuscript; available in PMC 2018 October 10.

Published in final edited form as:

Cancer Lett. 2017 October 10; 406: 71–80. doi:10.1016/j.canlet.2017.08.004.

Nanoemulsion Formulation of a Novel Taxoid DHA-SBT-1214 Inhibits Prostate Cancer Stem Cell-Induced Tumor Growth

Gulzar Ahmad[1], **Rana El Sadda**[2], **Galina Botchkina**[2,3], **Iwao Ojima**[2,4], **James Egan**[5], and **Mansoor Amiji**[1]

[1]Department of Pharmaceutical Sciences, School of Pharmacy, Northeastern University, Boston, Massachusetts 02115-5000

[2]Institute of Chemical Biology and Drug Discovery, Stony Brook University, Stony Brook, NY 11794-3400

[3]Department of Pathology, School of Medicine, Stony Brook University, Stony Brook, New York, 11794-8691

[4]Department of Chemistry, Stony Brook University, Stony Brook, New York, 11794-3400

[5]Targagenix, Inc., 25 Health Sciences Drive, Stony Brook, New York, 11790-3382

Abstract

The main aim of this study was to evaluate the therapeutic efficacy of an oil-in-water nanoemulsion formulation encapsulating DHA-SBT-1214, a novel omega-3 fatty acid conjugated taxoid prodrug, against prostate cancer stem cells. Nanoemulsions of DHA-SBT-1214 (NE-DHA-SBT-1214) were prepared and characterized. *In vitro* delivery efficiency and cytotoxicity of NE-DHA-SBT-1214 was compared with solution formulation in PPT2 cells. *In vivo* studies included analysis of comparative efficacy of NE-DHA-SBT-1214 with Abraxane® and placebo nanoemulsions as well as post-treatment alternations in clonogenic and sphere-forming capabilities of the tumor cells. Qualitative intracellular uptake studies of dye encapsulated NEs by confocal imaging showed uptake by both monolayer and spheroid cultured PPT2 cells. Treatment of PPT2 cells with NE DHA-SBT-1214 (1nM-1μM for monolayer culture of cells grown on collagen-coated dishes for 48 hrs.) induced complete cell death, showing higher efficacy as compared to the drug solution. This nanoemulsion (10nM-10μM) also showed toxicity in 3D

Corresponding author: Mansoor Amiji, PhD, Department of Pharmaceutical Sciences, School of Pharmacy, Northeastern University, Boston, Massachusetts 02115. Phone: 617-373-3137; Fax: 617-373-8886; m.amiji@northeastern.edu.

5. Conflicts of Interest

The authors declare no conflicts of interest.

6. Authors' Contributions

Conception and design: JE, IO, MA and GB
Development of methodology: GA, MA, RE, GB, IO, and JE
Acquisition of data: GA, RE, and GB
Analysis and interpretation of data: GA, RE, GB, MA, IO, and JE
Writing, review, and/or revision of the manuscript: GA, GB, MA, IO, and JE
Study supervision: MA, IO, JE, and GB

culture of floating spheroids. Weekly intravenous administration of the NE-DHA-SBT-1214 to NOD/SCID mice bearing subcutaneous PPT2 tumor xenografts led to dramatic suppression of tumor growth compared to Abraxane® and placebo nanoemulsion formulation. Viable cells that survived from this *in vivo* treatment regimen were no longer able to induce floating spheroids and holoclones, whereas control and Abraxane® treated tumor cells induced a large number of both. The results show that NE-DHA-SBT-1214 possesses significant activity against prostate $CD133^{high}/CD44+/^{high}$ tumor-initiating cells both *in vitro* and *in vivo.*

Keywords

Prostate Cancer; Cancer Stem Cells; Taxoid; Nanoemulsion Formulation

1. Introduction

Therapeutic options for treating cancer, affecting a large population of the United States are still very limited (1). In contrast to other human cancers, incidence and death rates of prostate cancer (PrCr) have significantly increased in the current decade (2). More than 70% of PrC patients will face post-treatment recurrence and transition of the disease to an incurable state (3). Similar to many other cancers, PrCr is also caused by a small population of malignant stem cells known as cancer stem cells (CSCs) or tumor-initiating cells (TICs), which are responsible for tumor development, metastasis, and resistance to anti-cancer therapies (4). Numerous studies on many cancer types have demonstrated that the tumorigenic cells expressing common CSC markers, in particular CD133 and CD44, are resistant to conventional anti-cancer drugs and these cells can propagate significantly after therapy (5). The mechanisms of drug resistance in CSCs are thought to be dependent on several factors including up-regulated expression of drug efflux transporters, the activation of anti-apoptotic signaling pathways, inactivation of apoptotic machinery, a state of quiescence, an enhanced DNA damage response and active repair mechanisms. Current prostate cancer treatments primarily target the bulk neoplastic, fast-growing cancer cells but not the CSCs subpopulation. This could provide the reason for the limited survival benefits seen with most prostate cancer therapies (6) and high failure rate of anticancer drugs during development (7). In particular, current anti-cancer drugs in development against prostate cancer have a significantly lower success rate as compared to other cancers (8). One of the reason of this lessened progress is the used of commercially available cell lines with high passage number as preclinical tool for evaluating candidates of anticancer agents. Because after growing for long time, these cells accumulate both genomic and epigenomic variable features and are dominated by a specific subpopulation which either has very low or no match with the original tumor (9). Therefore, use of these cell lines is not ideal for different applications, such as drug development, genomic alternation and to discover molecular drug targets. All of the above heeds, emphasis the need for better preclinical and physiological relevant *in vitro* and *in vivo* models to discover and develop drug targets for CSCs.

Our cell biology research laboratory has established patient-derived ultra-low passage prostate cancer cell line which stably retained the features of being immature and stem-like cells (PPT2 cell line) (10). Previous studies from this laboratory have demonstrated that the

$CD133^{high}/CD44^{high}$ phenotype of prostate cancer cells showed clear stem cell-related features, including high tumor- and spheroid-initiating capacities, plasticity, and high resistance to standard drugs (11). These cells express over-activated developmental pathways and express high levels of several key transcription factors, determining embryonic stem cell pluripotency. In addition, the PPT2 cells express many genes related to anti-apoptotic signaling and drug resistance, which make them a good model for CSC-targeted drug development studies.

Even though, two commonly used toxoids; Paclitaxel and docetaxel have shown some potential against different types of cancers, such as ovarian, lung, breast and prostate but are unable to cure these cancers due to multi-drug resistance (MDR) phenomenon of the tumor and nonspecific action of these drugs (12). To combat these concerns, scientists have developed different next generation taxoids (13, 14), which are 2–3 fold more potent than paclitaxel and docetaxel against MDR expressing drug-resistant cell lines (13, 14). One of these new generation toxoids, is SBT-1214, which has shown highest efficiency against drug-resistant (Pgp+) colon tumor xenografts in NOD/SCID mice (14) and was able to kill CSCs when used against colon CSCs from different cell lines, including HCT116, HT-29 and DLD-1 cell lines in 3D spheroid cultures assay (15). These results emphases the use SBT-1214 against PPT2 CSCs in this study.

In order to develop tumor specific chemotherapeutic drugs, SBT-1214 drug was conjugated with polyunsaturated fatty acids (PUFAs) because PUFAs improves their cancer-specific toxicity, has synergistic effects with cytotoxic drug, protects healthy cells, and decrease systemic toxicity. Among naturally occurring n-3 PUFAs, docosahexaenoic acid (DHA) exhibited the highest potency and has been studied extensively. For example, a DHA-paclitaxel conjugate, Taxoprexin® showed efficacy in Phase II clinical trials against prostate, breast, gastric, and lung cancers as well as metastatic melanoma (16) and advanced to phase III human clinical trials against metastatic melanoma (17). The DHA-SBT-1214 has shown better efficiency in mouse models of different types of tumor xenografts, including ovarian, colon, lung and pancreatic cancer (18, 19). However, in these studies, DHA-SBT-1214 was formulated in solutol HS-15 (or polysorbate 80)/ethanol/saline, and the use of an excipient was found to impose well-documented adverse effects, ascribed to the excipient and ethanol, as well as some stability issues at lower concentration of the excipient. Therefore, we have studied the efficacy of the nanoemulsion formulation developed in our research laboratory. Nanoemulsion based delivery of the anticancer drugs just like other nano-scale molecules, improve the “enhanced permeability and retention (EPR)” effect of the drug (20, 21). Even though, the accumulation of nanoemulsion does not require a specific receptor rather their EPR effect is passive in nature but still efficacious (22, 23). Our nanoemulsion formulation protocol includes phospholipids and fish oil. The use of DHA-SBT-1214 is advantageous in this formulation due to high affinity of this drug to the fish oil component that result in higher encapsulation efficiency, meaning high concentration of the drug inside nanoemulsion. In this *in vivo* study, we hypothesized that DHA-SBT-1214 in nanoemulsion formulation would be delivered to CSC-initiated PPT2 prostate tumor selectively via EPR effect, internalized to the cancer cells via endocytosis and will release SBT-1214 inside the cancer cells, which would cause apoptosis to tumor cells and then eradicate the tumor. The first line therapy for castration-resistant prostate cancer (CRPS) has been docetaxel with

prednisone, and cabazitaxel, which was approved by FDA in 2010 in place of or in addition to docetaxel treatment. However, CRPS involving CSCs does not exhibit androgen signaling and thus this type of CRPS is not responding to the combination of docetaxel or cabazitaxel with prednisone (24). Accordingly, it is worthwhile to investigate the efficacy of NE-DHA-SBT-1214 against patient-derived CSC-initiated prostate tumor xenografts in a mouse model.

2. Materials and Methods

2.1 Materials

New-generation taxoid, DHA-SBT-1214 was synthesized by ChemMaster International, Inc. (Stony Brook, NY). Extra pure omega-3 rich fish oil was purchased from Jedwards International (Quincy, MA), Lipoid E80 from Lipoid GMBH (Ludwigshafen, Germany), DSPE PEG2000 from Avanti Polar Lipids, Inc. (Alabaster, AL), Tween 80 from Sigma Chemicals, Inc. (St. Louis, MO), CellTiter 96 AQ_{ueous} one solution cell proliferation assay kit (G3580), from Promega (Madison, WI), Mesenchymal stem cell growth media (MSCGM) from Lonza (Portsmouth, NH), LAL chromogenic endotoxin quantitation kit from Thermo Scientific (Rockford, IL), Microscope slides single depression concave from Amscope (Irvine, CA), Collagenases type II and type IV from Sigma-Aldrich, Rhodamine 123 from Sigma Aldrich (St. Louis, MO), Anti-human CD133/2-APC antibody (clone 293C3) from Miltenyi Biotec, CA, USA; CD44-FITC antibody (clone F10-44-2) or CD44-PE antibody (clone F10-44-2) from; Invitrogen/Biosources, USA; CD166-PE antibody (clone 105902) and CD44v6-FITC antibody (clone 2F10) from; R&D Systems, MN, USA, EpCAM-FITC antibody from Biosource, CA, USA, Pan-Keratin (C11) antibody-Alexa Fluor® 488 from Cell Signaling and all the isotype controls antibodies were purchased from Chemicon. Penicillin, streptomycin and Trypsin-EDTA were obtained from Invitrogen (Grand Island, NY, USA). All other reagents were purchased through Fisher Scientific.

2.2 Preparation and Characterization of the Nanoemulsion Formulations

Preparation of nanoemulsion formulations was carried out as reported previously with some modifications (25). Instead of a sonication method, oil-in-water nanoemulsions were prepared by high pressure homogenization method. Briefly, pre-warmed oil phase (10ml) consisting of fish oil alone (for blank/placebo) or with DHA-SBT-1214 was gradually added to the pre-warmed water phase (40ml) containing egg phosphatidylcholine (Lipoid E80®) (1200mg), polysorbate 80 (Tween80®) (0.5ml), DSPE-PEG2000 (1, 2-distearoyl-Sn-glycero- 3- phosphoethanolamine- N- [amino (polyethylene glycol)-2000]) (150mg). The resultant mixture was homogenized and the oil-water suspension was passed through the zirconia plunger of a M-110EH-30 (Microfluidics, Inc., Westwood, MA) high shear fluid processor at 10,000 psi for 4 cycles to achieve a uniform nanoemulsion formulation. The oil-in water nanoemulsion formulation was characterized by well-established protocols in our laboratory (26). Drug loading, encapsulation efficiency and stability was evaluated using HPLC as described previously (27). All batches of nanoemulsions were tested for endotoxin level through Limulus Amebocyte Lysate (LAL) assay according to manufacturer's instructions before apply for both in vivo and in vitro studies.

2.3 Cell Culture, Isolation, Purification and Characterization of Tumor-Initiating Cells

The human prostate cancer stem cells (PPT2), prostate adenocarcinoma CSC-enriched cell line was established from the stage pT2c pNX pMX prostate cancer patient and cultured according to well established protocol (10). For cell culture from primary mouse tumors, tumor tissues were mechanically and enzymatically disaggregated into single cell suspension under sterile conditions, rinsed with Hank's balanced salt solution and incubated for 1.5 hours at 37°C in serum-free RPMI medium 1640 containing 200units/ml Collagenases type II and type IV, 120μg/ml penicillin and 100μg/ml streptomycin. Cells were further disaggregated by pipetting and serial filtration through cell dissociation sieves (size 40 and 80 meshes; Sigma-Aldrich). Primary cell suspensions were grown both as monolayer and in spheroids.

2.4 Cellular Uptake Studies

In order to evaluate and compare uptake of rhodamine encapsulated nanoemulsion formulation in both monolayer and spheroid cultured PPT2 cells, fluorescence confocal microscopy studies were performed as described previously (26). All setting parameters for fluorescence detection and analyses of images were held constant to allow consistency in imaging of the sample for comparison.

2.5 Cell Viability Analysis

The cell viability studies were performed with both aqueous drug solution and the nanoemulsion formulations containing different concentration of DHA-SBT-1214. For this purpose, PPT2 cells were seeded into collagen coated 96-well plates at a density of 10,000 cells per well. After 24 h, DHA-SBT-1214 in different concentrations was added to the monolayer cells either in aqueous solution or in nanoemulsion formulations along with respective controls. Following 48h incubation period, cell viability was determined with CellTiter assay according to manufacturer's instructions. The percent cell viability was calculated based on the absorbance of the drug-treated cells over the absorbance of control (media alone) cells and multiplied by one hundred. 50% inhibition of cell viability (IC_{50}) was calculated using Graph Pad Prism.

2.6 *In Vivo* Tumor Xenografts in NOD/SCID Mice

All experiments involving the use of animals were carried out in strict accordance with the recommendations in the Guide for the Care and Use of Laboratory Animals of the National Institutes of Health, via a research protocol that was approved by Stony Brook University Institutional Animal Care and Use Committee (IACUC) as described previously (10). Briefly, after sufficient propagation, clonogenic cells expressing high levels of CD133, CD44, CD44v6, CD166 and EpCAM were resuspended in 1:1 MSCGM/Matrigel and injected to the flanks of 6 weeks old NOD/SCID mice. The primary tumor sizes were measured with a caliper on a weekly basis and approximate tumor weights determined using the formula $0.5ab^2$, where b is the smaller of the two perpendicular diameters.

2.7 *In Vivo* Efficacy of NE-DHA-SBT-1214 and Abraxane® and *Ex Vivo* Characterization of Primary Tumor Cells

To compare therapeutic efficacy of different formulations, NE-DHA-SBT-1214 (1, 3, 10, 25, 30, 40, 50 and 70mg/kg) and Abraxane (30 and 40mg/kg) was administered intravenously on weekly basis for 3 weeks to NOD/SCID mice bearing palpable tumor xenografts. Treatment was started one week after transplantation of the PPT2 cells when tumor xenografts reached ~50–150mm^3. Systemic toxicity in NOD/SCID mice was closely monitored and evaluated by standard criteria (motor activity, morbidity, appetite, posture and appearance) and were humanely euthanized after they seemed moribund, or had too large or ulcerated tumors. After the last treatment, tumor development was monitored for an additional 4 weeks. All mice were terminated after four weeks of follow up. Some control or post-treatment residual tumors were harvested and analyzed histopathologically, for *ex vivo* clonogenic and sphere-forming capacities and other assays. For post treatment in vitro characterization, mouse tumor xenografts were harvested and disaggregated mechanically and enzymatically into single cell suspensions. The ability of these primary cells to induce round colonies (holoclones) and sphere formation was determined for both control (untreated) and drug treated mice. Some of these primary tumors cells from both untreated and drug treated mouse tumor xenografts were used for analysis of the drug-induced alterations in expression of different stem cell markers by FACS analysis.

2.8 Statistical data analysis

The in vitro response to different drug treatments was calculated on the basis of cell death of drug-treated versus untreated control cells. Whereas, the *in vivo* responses to drug treatment were evaluated as changes in tumor volume of drug-treated versus untreated control xenografts. Data were expressed as means ± SD for control and drug treated tumors. The statistical significance of differences was determined using Student's *t*-test with Graph Pad Prism® software (GraphPad Software, La Jolla, CA, USA). The parameters used were the two-tailed distribution and the paired test. $P<0.05$ was considered statistically significant.

3. Results

3.1 Characterization of DHA-SBT-1214 Nanoemulsion Formulation

Nanoemulsions are dispersions of two different liquids which are usually immiscible in each other. Depending on the order of adding liquid, these are either called water-in oil or oil-in-water and are nanometer in size. Nanoemulsion formulations are the most commonly used carriers for hydrophobic drug delivery, due to their effective therapeutic ability both *in vitro* and *in vivo*. Many anticancer drug encapsulated nanoemulsions have shown enhanced efficacy due to their target-specific systemic delivery to tumor site and EPR effect. This delivery approach has also shown enhanced therapeutic potential in our previous studies (26).

In current study, we have developed oil-in-water nanoemulsions using fish oil, which is rich in PUFAs such as omega-3 and omega-6 fatty acids and has the capability to solubilizes a significant amount of lipophilic anticancer drugs. The nanoemulsion formulation was used to encapsulate DHA-SBT-1214, a new generation taxoid as a stand-alone therapy against

prostate cancer. We used a microfluidic technique to yield a uniform, milky-white emulsion formulation (28). All the nanoemulsions were near spherical in structure with a size range of 100–220nm, as observed with transmission electron microscopy (TEM) (Fig. 1A). Particle size, polydispersity index (PDI) and zeta potential (surface charge) were determined for placebo, DHA-SBT-1214 loaded nanoemulsion formulations and Abraxane. All the formulations made by microfluidic technique and filtered through 0.2-micron filter had small size (< 230nm) and narrow PDI (< 0.3) except Abraxane® which has PDI of 0.361 and were negatively charged. Table S1 shows the average particle sizes, PDI and zeta potentials of all formulations used in the present study. Representative graphs of size and zeta potential of DHA-SBT-1214 nanoemulsion formulations are shown in Figure 1(B) and 1(C) respectively. The average particle size of the blank nanoemulsion (without any drug) was 225 ± 7nm. The incorporation of DHA-SBT-1214 in nanoemulsions did not significantly change the hydrodynamic particle size and it remained at approximately 228 ± 7nm. Abraxane showed smaller particle size compared to both nanoemulsion formulations. The average surface charge of the oil droplets in the nanoemulsions were in the range of −20.2 to −27.0mV. Surface charge of all the formulations was not significantly different employing the maximum encapsulation of the drug inside oil droplets. An HPLC assay was used to determine the drug concentrations in the nanoemulsion formulations. DHA-SBT-1214 nanoemulsion at 20mg/ml had the drug loading of 97%. This high drug encapsulation efficiency of nanoemulsions was attributed to the relative lipophilicity of the drugs, as these drugs retained in the oil core of the nanoemulsions. Additionally, all the formulations retained their particle size and surface charge during storage and drug encapsulated nanoemulsion formulations were chemically stable for up to 6 months upon storage at 4°C. All the formulations had minimum level of endotoxin as confirmed through Limulus Amebocyte Lysate (LAL) assay during storage period.

3.2 *In Vitro* Evaluations of NE DHA-SBT-1214 in PPT2 CSCs

To examine whether nanoemulsions were internalized in monolayer and in spheroids of PPT2 cells, rhodamine was encapsulated into nanoemulsions and confocal microscopy studies were performed. The optimal cell and spheroid uptake of rhodamine encapsulated nanoemulsion formulation was observed after 8 hours incubation with different concentrations of the dye formulations as shown in Fig. 2(A) and 2(B) respectively. The images from Figure 2 clearly indicate that the nanoemulsions do efficiently deliver the encapsulated dye in the cells and that the increased fluorescence signal at higher concentration of rhodamine nanoemulsion treated cells and spheroids indicates the higher intracellular uptake by PPT2 cells and spheroids. Since the internalization of nanoemulsion formulation was confirmed by cell uptake experiments, we replaced rhodamine with DHA-SBT-1214 in the nanoemulsion formulation and compared its effect on cell viability with drug solution. The cell-kill efficiency of DHA-SBT-1214 in aqueous solution and in the nanoemulsion formulations was examined in PPT2 cells monolayer using the CellTiter assay. The final concentrations of DHA-SBT-1214 selected for these studies were 1, 10, 100 and 1000nM based on study of SBT-1214 (6, 10, 29, 30). The dose-response studies against DHA-SBT-1214 as a single agent in PPT2 cells are summarized in Table S2 and shown in Fig. 3(A). The results are shown as percent viable cells remaining as a function of treatment following 48 hours of drug exposure at 37°C. When DHA-SBT-1214 was administered at 10

and 100nM concentrations, higher cytotoxicity was observed with the nanoemulsion formulation as compared to the aqueous solution. The IC_{50} of DHA-SBT-1214 solution for the PPT2 cells was 48nM, whereas the IC_{50} for the same cells with DHA-SBT-1214 nanoemulsion formulation was 4nM. This revealed that PPT2 cells needed at least ~12-fold higher concentration of DHA-SBT-1214 solution to achieve a similar IC_{50} as compared to its counterpart drug nanoemulsion formulation, demonstrating the superior efficacy of nanoemulsion formulation over drug solution.

In order to confirm if DHA-SBT-1214 nanoemulsion also kill PPT2 cell spheroids, we treated equal number of spheroids with different concentration of DHA-SBT-1214 nanoemulsion ranging from 0.01 to 10 μM and after specific time and observed their phenotype with bright field microscope (10). Figure 3B shows bright, healthy spheroids in the untreated sample which becomes dark brown with the increase in concentration displaying enhanced cell death by increasing the drug encapsulated nanoemulsion.

3.3 PPT2 Cell Line and CSC-Based *In Vivo* Xenograft Model

The vast majority of the recently established PPT2 cells (10), remains undifferentiated (only 3–5% express pan-keratin, a marker of differentiated cells) and possess many stem cell characteristics, including high levels of expression of many common cell surface markers, such as CD133, CD44, CD44v6, CD166, CD49f and EpCAM. In addition, the PPT2 cells express several markers of pluripotency, including c-Myc, Oct-4 and Sox-2 amongst others. These $CD133^+$ PPT2 cells also show some characteristic of embryonic and neural stem cells because of higher level of nestin and vimentin in their cytoplasm. About 10% of the total population of the PPT2 cells with the highest expressions of CD133 and CD44 co-expressed the highest levels of the CXCR4, the chemokine receptor associated with metastatic activity in several cancer types. However, these cells are resistant to traditional anticancer drugs and do not express p21 and p53 which are tumor suppressor proteins. The PPT2 cells stably possess very high clonogenic (holoclones), sphere-forming and tumorigenic capacities. In addition, these cells are extremely resistant to drug treatment. All of the above represents solid arguments for the utilization of the PPT2 cell line for evaluation of CSC-targeted efficacy of anticancer drug candidates. Although even several thousand of PPT2 cells uniformly induced tumors in NOD/SCID mice, we have determined that subcutaneous transplantation of relatively high number of cells (up to 1 million cells per mouse) induces tumor xenografts with unusually high percent of stem-like cells. Thus, if transplanted cells contained up to 98% of $CD133^+$ cells and 84% of $CD44^+$ cells (Fig. 4A), the primary cell suspension prepared from mice tumor xenografts contained up to 91% of $CD133^+$ cells and 78% of $CD44^+$ cells (Fig. 4B). All these features suggest that the PPT2 *in vivo* and *in vitro* models are suitable for testing the CSC-targeted activities of the NE-DHA-SBT-1214.

3.4 Growth Inhibition of PPT2 Tumors in NOD/SCID Mice

All animal procedures were carried out under the guidelines and approval of the institutional animal care and use committee (IACUC). After transplantation of the PPT2 cells, NOD/SCID mice were divided into particular number of groups for weekly treatment by intravenous injections of NE-DHA-SBT-1214 (25, 30, 40, 50 and 70mg/kg), Abraxane™ (25 and 40mg/kg; Abraxane™ is Cremophor® EL-free nanoparticle albumin-bound paclitaxel),

and vehicle (untreated control). Each dose group contained four mice (n=4; group treated with 25mg/kg of NE-DHA-SBT-1214 had n=6). Treatment was started one week after transplantation of the tumor cells, when tumor xenografts became palpable (tumors usually reached 50–150mm^3). Tumor development was monitored weekly. After 3 sets of weekly injections, tumor growth was monitored for additional 4 weeks, and all the measurements and morphology are presented in Fig. 5. We have found that in contrast to Abraxane (Fig. 5B, C), even relatively low concentrations of NE-DHA-SBT-1214 induced dramatic suppression of tumor growth (Fig. 5D, E, F) compared to untreated tumor xenografts (Fig. 5A), and dose dependent reduction of tumor volume compared to the initial tumor size (Fig. 5H). Thus, all tested concentrations of the NE-DHA-SBT-1214 induced tumor shrinkage. All the residual post-treatment tumors were virtually transparent, without a visible vascularization. Maximal tumor regression was observed by the 4th week of follow-up. In particular, 25mg/kg induced in average 45% shrinkage, 30mg/kg – 62%, 40mg/kg – 74% and 50mg/kg – 88% (Fig. S1) reduction of tumor volume. Of note, higher dose of NE-DHA-SBT-1214 (70mg/kg) (Fig. S1) did not augment tumor reduction. In contrast to NE-DHA-SBT-1214, the optimal dose of Abraxane (25mg/kg) and even 40mg/kg caused only insignificant suppression of the PPT2-induced tumor growth for about 4 weeks followed by continued growth at the rate similar to untreated mice xenografts (Fig. 5H). Although the tumor growth inhibition and tumor shrinkage in all mice treated with different concentrations of NE-DHA-SBT-1214 was dramatic, all mice lost up to 17% of body weight by third week of treatment (Fig. 5G and Fig S1B). However, from the second week of follow-up, all mice started to gain weight. No significant body weight changes were induced by treatment with Abraxane. Four weeks after the last treatment, the residual tumors from different experimental groups were harvested and subjected to histopathological, genomic and functional analyses. Untreated control tumors were removed on reaching a maximum dimeter of ~2 cm according to the requirements of IRB protocol.

3.5 Tissue Histopathological Analysis

We have analyzed the hematoxylin and eosin stained tumor xenografts tissue sections, as well as tissue sections of several major organs, including liver, kidney, intestine and pancreas, from the untreated and NE-DHA-SBT-1214 treated NOD/SCID mice. Control untreated tumor tissue sections show classic histologic features of human poorly differentiated adenocarcinoma with a great degree of nuclear atypia (Fig. 6A). The NE-DHA-SBT-1214 treated tumor tissues showed significant cellular abnormalities, profound hyalurization, vacuolization and extensive necrosis (Fig. 6B–D). Among histologically evaluated major organs, such as liver (Fig. 6E), kidney (Fig. 6I), intestine (Fig. 6G), pancreas (Fig. 6K), only liver tissue from NE-DHA-SBT-1214 treated mice showed reactive nuclear changes of hepatocytes, suggestive of some injury (Fig. 6F). Other organs did not show any diagnostic abnormalities (Fig. 6H, 6J and 6L).

3.6 Post-Treatment Alterations in Clonogenic and Sphere-Forming Capacities of Tumor Cells

To test whether or not treatment with NE-DHA-SBT-1214 affects the clonogenic potential of the CSC-enriched mice tumor xenograft cells, total cell suspensions from the control, and NE-DHA-SBT-1214-treated residual tumors (*ex vivo* cell culture) were seeded on type I

collagen-coated dishes and ULA plates. Untreated (vehicle-treated) PPT2-induced tumor xenografts were densely vascularized (Fig. S2A-1, A-2) and the NE-DHA-SBT-1214 treated residual tumors were very small, transparent, lacked visible capillaries (Fig. S2B-1, B-2) and did not produce adherent holoclones, with only sporadic appearance of a single spheroids in 3D cultures. These Primary tumor cells underwent profound cell death in the next several days in culture as shown by percent viable cell data of untreated spheroids (Fig. S2C) and NE-DHA-SBT-1214 treated spheroids (Fig. S2D), grown from primary tumor cell suspensions.

4. Discussion

It is largely documented that tumor initiating stem cells, along with being resistant to standard anticancer drugs are also able to promote progression of cancer and this progression is the result of increase in their self-renewal potential which is caused by drug-induced compensation (5, 31, 32). This highlights the need for effective therapeutic interventions targeting these CSCs. Previous studies were performed on patient-derived CSC-enriched PPT2 cell line, which maintain their stemness features (10). The observed over-activation of several developmental cascades in PPT2 cells from this study (10), was linked with regulation of prostate stem cell (33, 34), and androgen-independence metastasis progression of prostate cancer (35, 36). Further studies demonstrated the involvement of OCT3/4 and SOX2 in metastasis of prostate cancer (37) and association of nestin and vimentin with changeover from androgen-dependent to castration-resistant prostate cancer which is also metastatic (38, 39). Therefore, it would be beneficial to develop drugs targeting CSCs from the most aggressive tumor types or cell lines, because such drugs can potentially have a larger spectrum of mechanisms of action, and therefore, broader anti-cancer implications. Increasing evidence indicates that effective anticancer drugs should target cancer-specific tumor-initiating cells, which are functionally and morphologically different from their bulk tumor counterparts. Above discussion proposes that the PPT2 cells will serve as an ideal model not only for functional studies of prostate cancer but also for cancer stem cell targeted drug development.

It was recently shown that drugs targeting major stem cell signaling pathways, such as Hedgehog and Notch, induce serious side effects on normal stem cells (40). The inhibition of the drug efflux pumps in attempt to modulate drug resistance of CSCs did not provide any significant clinical benefit (41). Accumulating clinical and preclinical evidence indicated that the benefits of antiangiogenic agents to the long-term survival of cancer patients was negligible (42). For example, docetaxel and paclitaxel might treat patients with androgen-independent prostate cancer in the beginning, but the cancer comes back more aggressively due to some flaws of these taxoids (3, 43). Somehow, paclitaxel is still a front-line treatment for many solid tumor (44, 45), it initiates the apoptosis and causes cell cycle arrest at the G2/M stage (46, 47). To further improve the efficiency of paclitaxel, numerous formulations as well as prodrugs of paclitaxel have been developed that increase its aqueous solubility, such as cyclodextrin, lipsomes and HSA-bound nanoparticle (“Abraxane”) formulations (17). However, some cancers including colon and prostate overexpress P-glycoprotein (Pgp), an effective ATP-binding cassette (ABC) transporter and effluxes paclitaxel, that is why paclitaxel is not effective against these cancers (12). In order to overcome efflux issue,

Paclitaxel was conjugated with DHA, because DHA conjugated drug has higher affinity for human serum albumin (HAS) which is the primary carrier for PUFAs in the bloodstream (48). From this study, it was concluded that when DHA is conjugated to paclitaxel, it becomes a weak substrate for Pgp as compared to free paclitaxel but in cancers which overexpress Pgp and/or other ABC transporters, when paclitaxel free itself from DHA in the presence of esterase, even though it will be released slowly but still be caught by the efflux pump(s) and eliminated from the cancer cells (48). Along with paclitaxel, Marin-Aguilera et al., has reported that docetaxel can also de-differentiate prostate cancer cells through TGF-β mechanism and induce drug resistance (49).

In contrast to paclitaxel, a new-generation taxoid, named SBT-1214, showed excellent activity against drug-resistant cancer cells, which express MDR phenotypes (12). Previously it has shown that this new-generation taxoid SBT-1214 induced long-term regression and tumor growth delay of drug-resistant colon tumor xenografts (48). Later on, another study concluded that SBT-1214 induced significant down-regulation of key transcription factors which are involved in stem cell regulation, progression and development of cancer (11). In order to enhance blood circulation and ultimately therapy, we have used DHA conjugated SBT-1214 in our current study.

To further improve delivery of this hydrophobic drug, we encapsulated DHA-SBT-1214 in nanoemulsions and reduced its particle size upto nanometer length through high shear stress of microfluidizing instruments (28). After encapsulation of DHA-SBT-1214 in nanoemulsion, the pharmacokinetic and biodistribution pattern of the drug is dictated by properties of the nanoemulsion instead of encapsulated drug characteristics. As an example, the PEG-modified nanoemulsions can enhance the longevity of the drug in the blood circulation. This in turn increases accumulation of drug at the tumor site through the EPR effect (50), but do not affect its physio-chemical properties. In current study, PEG surface modification of nanoemulsions using DSPE-PEG2000 did not affect the particle size, size distribution and surface charge values of the nanoemulsions. The qualitative cellular uptake analysis demonstrated that the nanoemulsion formulations were efficiently internalized in PPT2 cells and spheroids. This suggests that the nanoemulsions do efficiently deliver the payload to the subcellular sites in the cell and was more potent than its drug solution. In this study, we found that DHA-SBT-1214 suppress PPT2 tumors more when delivered in nanoemulsion formulations. In addition to these observations, flow cytometry analysis also revealed that implanted tumor cells retained their stemness inside the subcutaneous tumors. Therapy with DHA-SBT-1214 delivered in nanoemulsions indeed showed higher therapeutic efficacy in PPT2 cells and tumors. No significant body weight loss was observed in any of the treatment groups analyzed. Tissue histology did not show any abnormal findings in liver, heart or kidney from any of the treatment groups. These tests suggest that DHA-SBT-1214, when administered as nanoemulsion is well tolerated in mice. In conclusion, our data demonstrate that nanoemulsion of the DHA-SBT-1214 conjugate induces superior regression and tumor growth inhibition and has high potential as a novel CSC-targeted anti-cancer drug candidate.

Supplementary Material

Refer to Web version on PubMed Central for supplementary material.

Acknowledgments

Grant Support

Financial support was provided by the National Cancer Institute of the National Institutes of Health through grants and contract R21-CA150085 (to GB), R01-CA103314 and R44-CA132396 (to IO), HHSN261201500018C (to JE) and U01-CA151452 and R21-CA179652 (to MA).

Other Acknowledgements

Transmission electron microscopy of the nanoemulsion samples was performed by Mr. William Fowle at the Electron Microscopy Center, Northeastern University (Boston, MA). The authors thank Dr. Thomas Zimmerman, Director, Division of Laboratory Animal Resources (DLAR) at Stony Brook University (Stony Brook, NY) for his helpful advice and cooperation.

References

1. Siegel RL, Miller KD, Jemal A. Cancer statistics, 2016. CA Cancer J Clin. 2016; 66(1):7–30. [PubMed: 26742998]
2. Zhou CK, Check DP, Lortet-Tieulent J, Laversanne M, Jemal A, Ferlay J, et al. Prostate cancer incidence in 43 populations worldwide: An analysis of time trends overall and by age group. International journal of cancer. 2016; 138(6):1388–400. [PubMed: 26488767]
3. Jemal A, Bray F, Center MM, Ferlay J, Ward E, Forman D. Global cancer statistics. CA: a cancer journal for clinicians. 2011; 61(2):69–90. [PubMed: 21296855]
4. Reya T, Morrison SJ, Clarke MF, Weissman IL. Stem cells, cancer, and cancer stem cells. Nature. 2001; 414(6859):105–11. [PubMed: 11689955]
5. Konrad CV, Murali R, Varghese BA, Nair R. The role of cancer stem cells in tumor heterogeneity and resistance to therapy. Can J Physiol Pharmacol. 2017; 95(1):1–15. [PubMed: 27925473]
6. Ni J, Cozzi P, Hao J, Duan W, Graham P, Kearsley J, et al. Cancer stem cells in prostate cancer chemoresistance. Curr Cancer Drug Targets. 2014; 14(3):225–40. [PubMed: 24720286]
7. Hutchinson L, Kirk R. High drug attrition rates--where are we going wrong? Nature reviews Clinical oncology. 2011; 8(4):189–90.
8. Zhu L, Gibson P, Currle DS, Tong Y, Richardson RJ, Bayazitov IT, et al. Prominin 1 marks intestinal stem cells that are susceptible to neoplastic transformation. Nature. 2009; 457(7229):603–7. [PubMed: 19092805]
9. Gillet JP, Calcagno AM, Varma S, Marino M, Green LJ, Vora MI, et al. Redefining the relevance of established cancer cell lines to the study of mechanisms of clinical anti-cancer drug resistance. Proc Natl Acad Sci U S A. 2011; 108(46):18708–13. [PubMed: 22068913]
10. Botchkina GI, Zuniga ES, Rowehl RH, Park R, Bhalla R, Bialkowska AB, et al. Prostate cancer stem cell-targeted efficacy of a new-generation taxoid, SBT-1214 and novel polyenolic zinc-binding curcuminoid, CMC2.24. PloS one. 2013; 8(9):e69884. [PubMed: 24086245]
11. Botchkina GI, Zuniga ES, Das M, Wang Y, Wang H, Zhu S, et al. New-generation taxoid SB-T-1214 inhibits stem cell-related gene expression in 3D cancer spheroids induced by purified colon tumor-initiating cells. Molecular cancer. 2010; 9:192. [PubMed: 20630067]
12. Vredenburg MR, Ojima I, Veith J, Pera P, Kee K, Cabral F, et al. Effects of orally active taxanes on P-glycoprotein modulation and colon and breast carcinoma drug resistance. J Nat'l Cancer Inst. 2001; 93:1234–45. [PubMed: 11504769]
13. Ojima I, Wang T, Miller ML, Lin S, Borella C, Geng X, et al. Syntheses and Structure-Activity Relationships of New Second-Generation Taxoids. Bioorg Med Chem Lett. 1999; 9:3423–8. [PubMed: 10617084]

14. Ojima I, Chen J, Sun L, Borella CP, Wang T, Miller ML, Lin S, Geng X, Kuznetsova L, Qu C, Gallagher G, Zhao X, Zanardi I, Xia S, Horwitz SB, StClair JM, Guerriero JL, Bar-Sagi D, Veith JM, Pera P, Bernacki RJ. Design, Synthesis, and Biological Evaluation of New-Generation Taxoids. J Med Chem. 2008; 51:3203–21. [PubMed: 18465846]
15. Botchkina GI, Zuniga ES, Das M, Wang Y, Wang H, Zhu S, Savitt AG, Rowehl RA, Leyfman Y, Ju J, Shroyer K, Ojima I. New-generation taxoid SB-T-1214 inhibits stem cell-related gene expression in 3D cancer spheriods induced by purified colon tumor-initiating cells. Mol Cancer. 2010; 9:192–204. [PubMed: 20630067]
16. Jones RJH, RE, Eatock MM, Ferry DR, Eskens FALM, Wilke H, Evans TRJ. A phase II open-label study of DHA-paclitaxel (Taxoprexin) by 2-h intravenous infusion in previously untreated patients with locally advanced or metastatic gastric or oesophageal adenocarcinoma. Cancer Chemo Pharmacol. 2008; 61:435–41.
17. Hennenfent KLGR. Novel formulations of taxanes: a review. Old wine in a new bottle? Annals of Oncology. 2006; 17:735–49. [PubMed: 16364960]
18. Seitz, J., Ojima, I. Drug Conjugates with Polyunsaturated Fatty Acids. In: Kratz, F.Senter, P., Steinhagen, H., editors. Drug Delivery in Oncology – From Research Concepts to Cancer Therapy. Vol. 3. Weinheim: Wiley-VCH; 2011. p. 1323-60.
19. Kuznetsova LV, Chen J, Sun L, Wu X, Pepe A, Veith JM, et al. Syntheses and Evaluation of Novel Fatty Acid-2nd-generation Taxoid Conjugates as Promising Anticancer Agents. Bioorg Med Chem Lett. 2006; 16:974–7. [PubMed: 16298526]
20. Maeda, H., Matsumura, Y., Oda, T., Sasamoto, K. Cancer selective macromolecular therapeutics: tailoring of an antitumor protein drug. In: Feeny, RE., Whitaker, JR., editors. Protein Tailoring for Food and Medical Uses. New York: Marcel Dekker, Inc; 1986. p. 353-82.
21. Maeda H, Fang J, Inutsuka T, Kitamoto Y. Vascular Permeability Enhancement in Solid Tumor: Various Factors, Mechanism Involved and its Implications. Int Immunopharmacol. 2003; 3:319–28. [PubMed: 12639809]
22. van Vlerken LE, Duan Z, Seiden MV, Amiji MM. Modulation of Intracellular ceramide using polymeric nanoparticles to overcome multidrug resistance in cancer. Cancer Res. 2007; 67(10): 4843–50. [PubMed: 17510414]
23. Davis ME, Chen ZG, Shin DM. Nanoparticle therapeutics: an emerging treatment modality for cancer. Nat Rev Drug Discov. 2008; 7:771–82. [PubMed: 18758474]
24. Rane JK, Pellacani D, Maitland NJ. Advanced prostate cancer—a case for adjuvant differentiation therapy. Nat Rev Urol. 2012; 9(10):595–602. [PubMed: 22890299]
25. Kadakia E, Shah L, Amiji MM. Mathematical Modeling and Experimental Validation of Nanoemulsion-Based Drug Transport across Cellular Barriers. Pharmaceutical research. 2017
26. Ganta S, Amiji M. Coadministration of Paclitaxel and curcumin in nanoemulsion formulations to overcome multidrug resistance in tumor cells. Molecular pharmaceutics. 2009; 6(3):928–39. [PubMed: 19278222]
27. Shah L, Gattacceca F, Amiji MM. CNS delivery and pharmacokinetic evaluations of DALDA analgesic peptide analog administered in Nano-sized oil-in-water emulsion formulation. Pharmaceutical research. 2014; 31(5):1315–24. [PubMed: 24297071]
28. Sarker DK. Engineering of nanoemulsions for drug delivery. Curr Drug Deliv. 2005; 2(4):297–310. [PubMed: 16305433]
29. van Vlerken LE, Duan Z, Seiden MV, Amiji MM. Modulation of intracellular ceramide using polymeric nanoparticles to overcome multidrug resistance in cancer. Cancer research. 2007; 67(10):4843–50. [PubMed: 17510414]
30. Desai A, Vyas T, Amiji M. Cytotoxicity and apoptosis enhancement in brain tumor cells upon coadministration of paclitaxel and ceramide in nanoemulsion formulations. J Pharm Sci. 2008; 97(7):2745–56. [PubMed: 17854074]
31. Bao S, Wu Q, Sathornsumetee S, Hao Y, Li Z, Hjelmeland AB, et al. Stem cell-like glioma cells promote tumor angiogenesis through vascular endothelial growth factor. Cancer research. 2006; 66(16):7843–8. [PubMed: 16912155]

32. Bertolini G, Roz L, Perego P, Tortoreto M, Fontanella E, Gatti L, et al. Highly tumorigenic lung cancer CD133+ cells display stem-like features and are spared by cisplatin treatment. Proc Natl Acad Sci U S A. 2009; 106(38):16281–6. [PubMed: 19805294]
33. Birnie R, Bryce SD, Roome C, Dussupt V, Droop A, Lang SH, et al. Gene expression profiling of human prostate cancer stem cells reveals a pro-inflammatory phenotype and the importance of extracellular matrix interactions. Genome Biol. 2008; 9(5):R83. [PubMed: 18492237]
34. Bisson I, Prowse DM. WNT signaling regulates self-renewal and differentiation of prostate cancer cells with stem cell characteristics. Cell Res. 2009; 19(6):683–97. [PubMed: 19365403]
35. Verras M, Sun Z. Roles and regulation of Wnt signaling and beta-catenin in prostate cancer. Cancer letters. 2006; 237(1):22–32. [PubMed: 16023783]
36. Hall CL, Zhang H, Baile S, Ljungman M, Kuhstoss S, Keller ET. p21CIP-1/WAF-1 induction is required to inhibit prostate cancer growth elicited by deficient expression of the Wnt inhibitor Dickkopf-1. Cancer research. 2010; 70(23):9916–26. [PubMed: 21098705]
37. Bae KM, Parker NN, Dai Y, Vieweg J, Siemann DW. E-cadherin plasticity in prostate cancer stem cell invasion. American journal of cancer research. 2011; 1(1):71–84. [PubMed: 21968440]
38. Kleeberger W, Bova GS, Nielsen ME, Herawi M, Chuang AY, Epstein JI, et al. Roles for the stem cell associated intermediate filament Nestin in prostate cancer migration and metastasis. Cancer research. 2007; 67(19):9199–206. [PubMed: 17909025]
39. Zhao Y, Yan Q, Long X, Chen X, Wang Y. Vimentin affects the mobility and invasiveness of prostate cancer cells. Cell Biochem Funct. 2008; 26(5):571–7. [PubMed: 18464297]
40. Kaiser J. The cancer stem cell gamble. Science. 2015; 347(6219):226–9. [PubMed: 25593170]
41. Fletcher JI, Haber M, Henderson MJ, Norris MD. ABC transporters in cancer: more than just drug efflux pumps. Nature reviews Cancer. 2010; 10(2):147–56. [PubMed: 20075923]
42. Schmid BC, Oehler MK. Improvements in progression-free and overall survival due to the use of anti-angiogenic agents in gynecologic cancers. Curr Treat Options Oncol. 2015; 16(1):318. [PubMed: 25750175]
43. Zivi A, Massard C, De-Bono J. Changing therapeutic paradigms in castrate-resistant prostate cancer. Clin Genitourin Cancer. 2010; 8(1):17–22. [PubMed: 21208851]
44. Rowinsky EK. The development and clinical utility of the taxane class of antimicrotubule chemotherapy agents. Annu Rev Med. 1997; 48:353–74. [PubMed: 9046968]
45. McGuire WP, Rowinsky EK, Rosenshein NB, Grumbine FC, Ettinger DS, Armstrong DK, et al. Taxol: a unique antineoplastic agent with significant activity in advanced ovarian epithelial neoplasms. Ann Intern Med. 1989; 111(4):273–9. [PubMed: 2569287]
46. Schiff PB, Horwitz SB. Taxol stabilizes microtubules in mouse fibroblast cells. Proc Natl Acad Sci U S A. 1980; 77(3):1561–5. [PubMed: 6103535]
47. Jordan MA, Toso RJ, Thrower D, Wilson L. Mechanism of mitotic block and inhibition of cell proliferation by taxol at low concentrations. Proc Natl Acad Sci U S A. 1993; 90(20):9552–6. [PubMed: 8105478]
48. Kuznetsova L, Chen J, Sun L, Wu X, Pepe A, Veith JM, et al. Syntheses and evaluation of novel fatty acid-second-generation taxoid conjugates as promising anticancer agents. Bioorg Med Chem Lett. 2006; 16(4):974–7. [PubMed: 16298526]
49. Marin-Aguilera M, Codony-Servat J, Kalko SG, Fernandez PL, Bermudo R, Buxo E, et al. Identification of docetaxel resistance genes in castration-resistant prostate cancer. Molecular cancer therapeutics. 2012; 11(2):329–39. [PubMed: 22027694]
50. Maeda H, Wu J, Sawa T, Matsumura Y, Hori K. Tumor vascular permeability and the EPR effect in macromolecular therapeutics: a review. J Control Release. 2000; 65(1–2):271–84. [PubMed: 10699287]

Highlights

- Novel docosahexaenoic acid (DHA)-conjugated taxoid SBT-1214 was synthesized and encapsulated in fish oil-containing nanoemulsion.
- DHA-SBT-1214 nanoemulsion showed improved cell-kill efficacy *in vitro* in PPT2 human prostate cancer cells with cancer stem cell (CSC)-like phenotype.
- DHA-SBT-1214 nanoemulsion showed improved therapeutic efficacy *in vivo* in PPT2 tumor xenografts upon intravenous administration.
- Viable cells that survived DHA-SBT-1214 treatment from explanted *in vivo* xenograft were no longer able to induce floating spheroids and holoclone formation characteristics of CSC.

Figure 1A

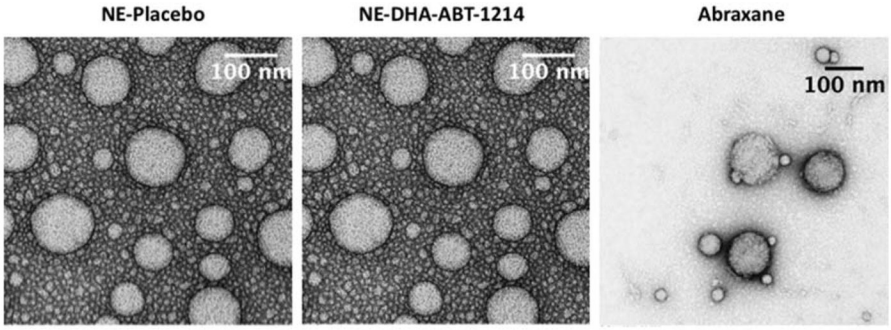

Figure 1B

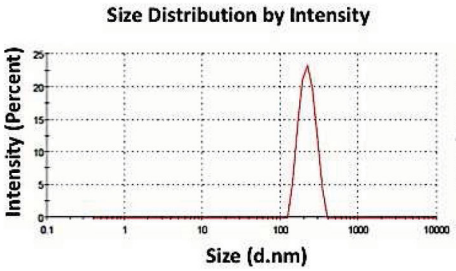

Figure 1C

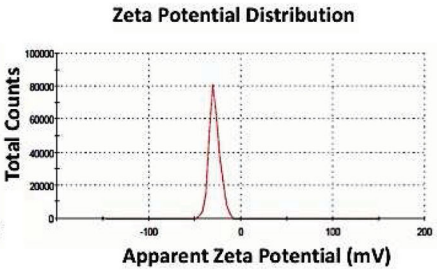

Figure 1. Characterization of DHA-SBT-1214 nanoemulsion formulation

1(A) – The transmission electron micrograph (TEM) of the placebo (NE-Placebo), DHA-SBT-1214 nanoemulsion formulation (NE-DHA-SBT-1214) and Abraxane. In the TEM image, both NE-Placebo and NE-DHA-SBT-1214 were taken at 60000x magnification but Abraxane was taken at 40000x magnification. The oil droplets of the nanoemulsion sample were spherical, and their size was in the range of 100–220 nm. The scale bar represents a distance of 100 nm. **1(B) –** Graph of particle size determination in nm; **1(C) –** Graph of zeta potential determination in mV.

Figure 2A

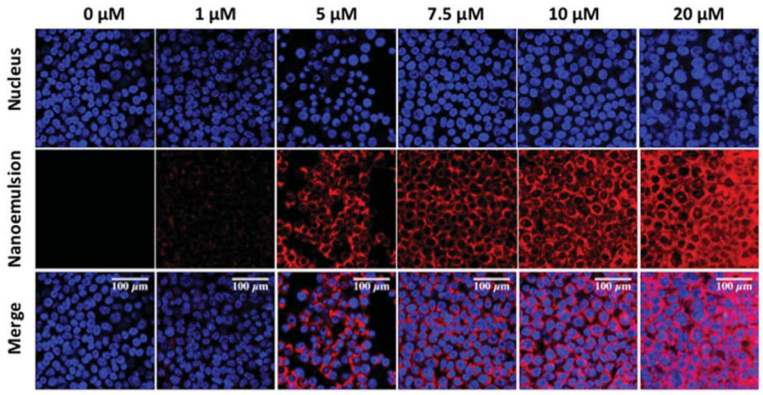

Figure 2B

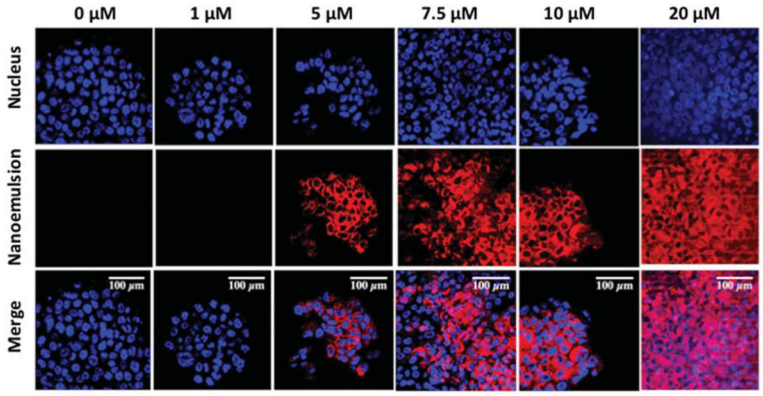

Figure 2. The uptake of rhodamine-encapsulated nanoemulsion formulation in monolayer 2(A) – and spheroid 2(B) – in PPT2 cell culture

Fluorescence microscopy images showing the blue (nucleus), red (rhodamine encapsulated nanoemulsion) and overlay images in purple color. The images were taken at 63x magnification. The image scale bar is 100 μm.

Figure 3A

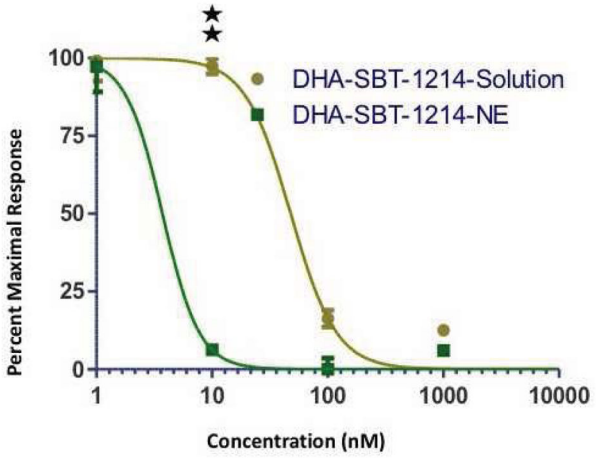

Figure 3B

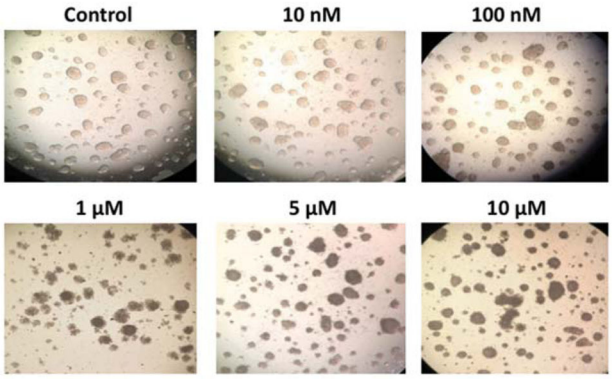

Figure 3. DHA-SBT-1214 solution and nanoemulsions activity in cells

3 (A) – The percentage maximal response as a function of DHA-SBT-1214 when administered in aqueous solution or in nanoemulsion formulations to PPT2 cells. The cell viability was measured by the CellTiter cell viability assay after 48h of incubation at 37°C. Data represent mean±standard deviation (n=3). Significant differences are indicated as follows: *P<0.05, and **P<0.01; **3(B) –** PPT2 spheroids were treated with different concentrations of DHA-SBT-1214 nanoemulsions and observed under microscope for toxicity.

Figure 4A

Transplanted PPT2 cells

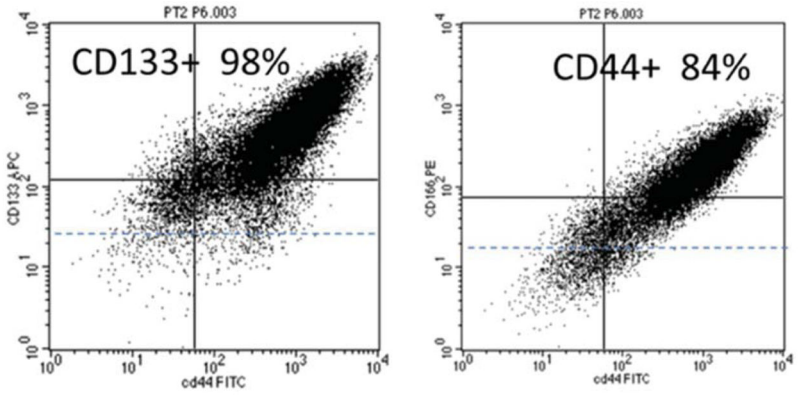

Figure 4B

Primary xenografts tumor cell suspension

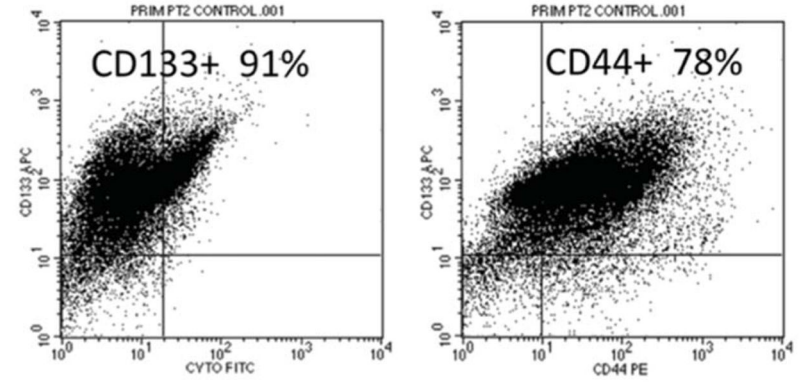

Figure 4. PPT2 cells retain their stem cell characteristic in tumor xenografts

(**4A)–** Flow cytometry analysis of cell surface markers expression in parental PPT2 cell line and (**4B)–** primary cell suspension from PPT2-induced mice tumor xenografts.

Figure 5G

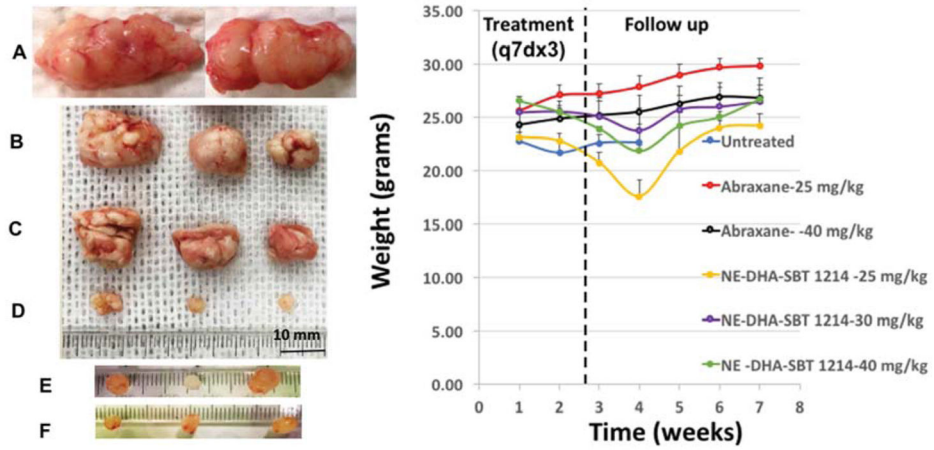

Figure 5H

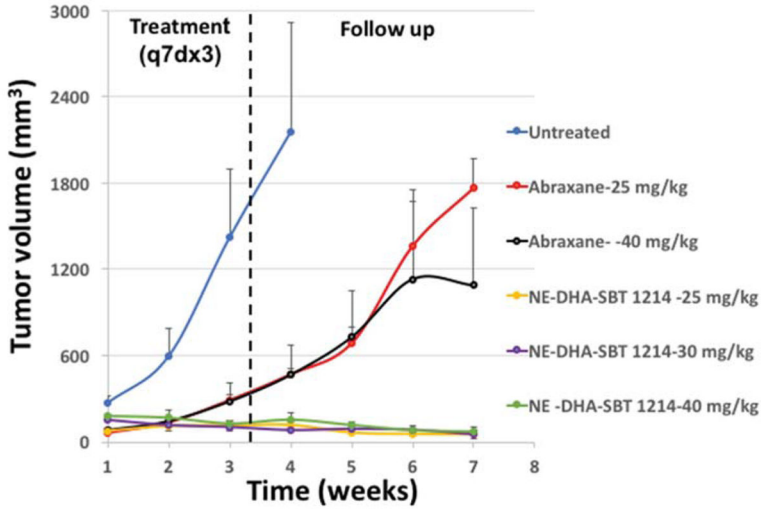

Figure 5. *In vivo* efficacy of the NE-DHA-SBT and Abraxane® against PPT2 induced mice tumor xenografts

(A) – control tumors from mice treated with vehicle; **(B, C)** – tumors from Abraxane® treated mice (25 and 40 mg/kg, respectively); **(D, E, F)** – tumors from NE-DHA-SBT treated mice (25, 30 and 40 mg/kg, respectively); **(G)** – body weight alterations induced by treatment with different concentrations of NE-DHA-SBT; **(H)** – graph summarizing all treatment modalities. The values are means±SD (n=4). Significant differences are indicated as follows: *P<0.05, and **P<0.01.

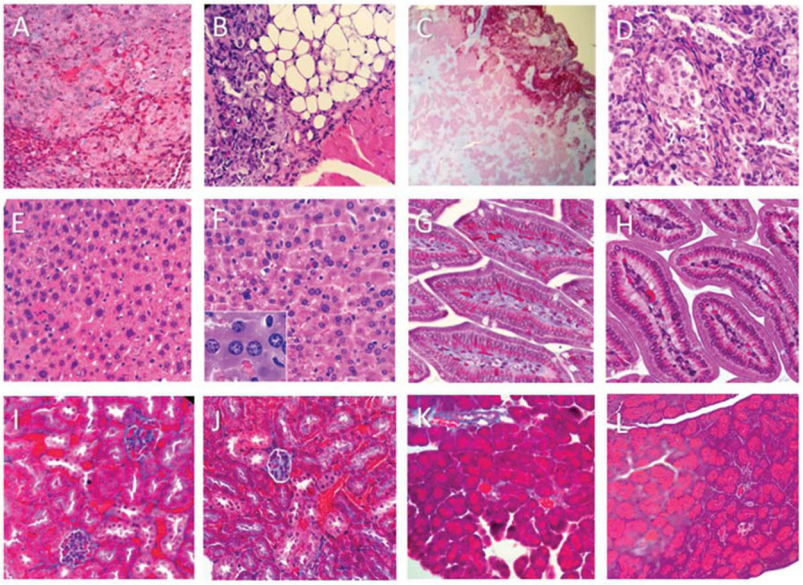

Figure 6. Histopathological evaluation of the PPT2-induced tumor and different organ tissues collected from control and NE-DHA-SBT treated mice (hematoxylin & eosin staining)

(A) – control untreated tumor shows poorly differentiated adenocarcinoma; (**B–D)** – 30 mg/kg NE-DHA-SBT-1214 treated tumor show massive hyalurization, vacuolization and extensive necrosis. Tissues form control untreated mice: **(E)** – liver; **(G)** – intestine; **(I) –** kidney; **(K)** – pancreas. Tissues from 40 mg/kg NE-DHA-SBT treated mice: (**F) –** liver (x40 in insert); **(H)** – intestine; **(J)** – kidney; **(L) –** pancreas. Note that only hepatocytes express some reactive nuclear abnormalities suggestive of injury (**F)**. No diagnostic abnormalities were detected in all other tested organs.